2018

Empirical Study on The Heat Exchange Effectiveness of A Cross-flow Thermoelectric Air To Air Heat Pump Unit

Seongyong Cheon
Hanyang University, Korea, Republic of (South Korea), csy5104@naver.com

Jae-Weon Jeong
Hanyang university, Korea, Republic of (South Korea), jjwarc@hanyang.ac.kr

Empirical Study on The Heat Exchange Effectiveness of A Cross-flow Thermoelectric Air To Air Heat Pump Unit

Seong-Yong Cheon, Jae-Weon Jeong*

Department of Architectural Engineering, Hanyang University,
Seoul, 04763, Republic of Korea
Contact Information (+8222202370, +82222201945, jjwarc@hanyang.ac.kr)

* Corresponding Author

ABSTRACT

Thermoelectric module (TEM) non-vapor-compression heat pumps are of interest as substitutes for conventional vapor-compression heat pumps. However, the heat exchange effectiveness and performance of TEMs for application to heating, ventilation, and air conditioning (HVAC) systems had been less studied. The purpose of this research is to propose the system configuration of TEM heat pump unit and to predict the heat exchange effectiveness in air heat pump system using TEM. The proposed system is composed by flat plate fin array that is heat exchanger integrated TEM for cooling and heating. The experiments were conducted to predicting the cooling and heating heat exchange effectiveness by collecting performance data. The performance data are composed by the inlet air fluid temperature, air flow rates at each side, heat exchange area, and input direct current (DC) to the TEM. Outlet fluid temperatures and TEM surface temperature are also measured for deriving the heat exchange effectiveness. Design parameters had significant impact on the heat exchange effectiveness of the flat plate heat exchanger integrated TEM for air cooling and heating. Consequently, in this paper, the influence of the five input parameters (air temperature at both side, air flow rate at both side, current) were analyzed. In proposed unit, the heat exchange effectiveness of hot and cold sides was 0.41 to 0.59 and 0.23 to 0.30, respectively.

1. INTRODUCTION

Thermoelectric module (TEM) non-vapor-compression heat pumps have been studied for application to air conditioning and ventilation systems in buildings. TEM heat pumps do not require refrigerants, produce no noise, have no moving parts, are of compact size, and exhibit a long lifetime, and thus are of interest as substitutes for conventional vapor-compression heat pumps (Al-Nimr et al., 2015). Several studies have investigated the potential of TEMs for air cooling and heating applications. Shen et al. (2013) studied a thermoelectric radiant air conditioning (TE-RAC) system, in which a TEM was applied as a radiant cooling device instead of conventional hydronic panels. With an applied current of 1.2 A, the maximum cooling coefficient of performance (COP) of the TE-RAC reached 1.77, as determined by simulation. Irshad et al. (2017) studied a thermoelectric air duct system, which is an air cooling system for controlling indoor air conditioning in a tropical climate, with a combined photovoltaic wall. The study demonstrated the feasibility of a TEM combination with renewable energy, thereby reducing energy consumption and eliminating the need for fossil fuels. Li et al. (2009) proposed a thermoelectric domestic-ventilation system, which was combined with a sensible heat exchanger. The research demonstrated the possibility of building a compact size ventilation system by using a TEM to minimize the size of the heat pump. The experimental results gave a COP of 2.5 for the proposed system. Kim et al. (2014) applied a thermoelectric module as a heating device in a building. As the TEM is a sort of solid heat pump, previous research has shown that TEMs can be considered for simultaneous cooling and heating in buildings. Yilmazoglu (2016) proposed a prototype thermoelectric air-to-air heating and cooling unit and analyzed experimental and numerical results from their investigation. This research showed the effects of air velocity and the psychrometric properties of TEM voltage differences. Lim et al. (2018) gave an empirical analysis for a water-to-water thermoelectric module, and their experimental results enabled them to construct a simplified non-dimensional model for a water-to-water thermoelectric heat pump unit that could be used for a

simultaneous cooling and heating system in a building. In addition, when a TEM is used for simultaneous cooling and heating in an HVAC system, the whole system integrated TEM offered a higher energy efficiency than that for a conventional system.
However, very limited studies have investigated the heat transfer characteristics and behaviors of a thermoelectric heat pump. Consequently, in this study, the impact of each design parameter and interactions between parameters were evaluated by using experimental results.

2. A CROSS-FLOW THERMOELECTRIC HEAT PUMP UNIT

In this section, we describe the general properties of a TEM and a configuration of an air-to-air thermoelectric heat pump (TEHP) unit as an air-to-air solid heat pump unit.

2.1 Thermoelectric module

Figure 1 shows the simultaneous cooling and heating at each side of the TEM. When direct current (DC) is applied to the TEM, the temperature of one side (the hot side) is increased and that of the other side (the cold side) is decreased. The temperature difference is proportional to the intensity of the current, and the temperature difference generated depends on the performance of the thermoelectric device. As a type of solid-state heat pump, the TEM has advantages of small size and low failure rate owing to the lack of fluid and refrigerant used for heat transfer.

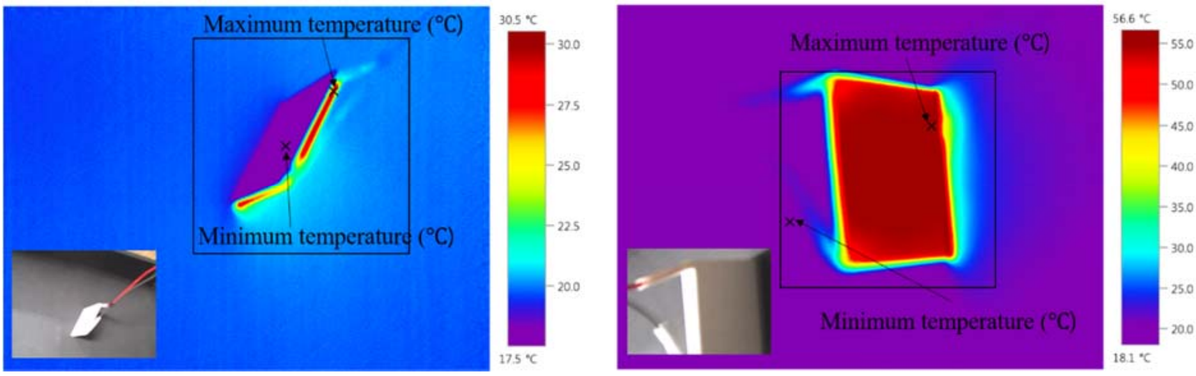

a. Cold-side temperature distribution b. Hot-side temperature distribution

Figure 1: Temperature distribution on each side of the thermoelectric module

Figure 2 shows the configuration of the thermoelectric element, which is composed of n-type and p-type semiconductors, and the Peltier effect. The Peltier effect refers to heat generation and heat dissipation when current is applied to two different conductors, as poles and electrons have a certain directionality. When the direction of the direct current is reversely applied, the heat-absorbing portion and the heat-emission portion are changed. Therefore, both a cooling and a heating device can be obtained by using single TEM. The heat absorption amount, heat radiation amount, and power of a TEM, respectively, can be obtained by

$$Q_c = SIT_c - \frac{1}{2}I^2R - K(T_h - T_c), \tag{1}$$

$$Q_h = SIT_c + \frac{1}{2}I^2R - K(T_h - T_c), \tag{2}$$

$$P = Q_h - Q_c = I^2R + SI(T_h - T_c). \tag{3}$$

The values of the Seebeck coefficient (S), thermal conductivity (K), and electric resistance (R) are determined according to the performance of the thermoelectric element, which affects the amount of heat dissipation, heat absorption, and electric power of the TEM.

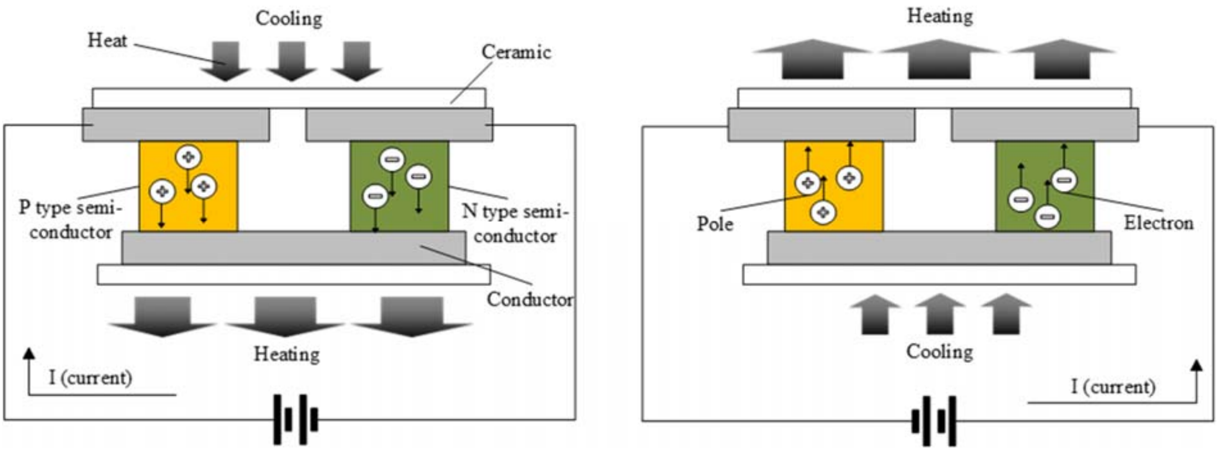

Figure 2: Schematic of the thermoelectric element and the Peltier effect

2.2 Cross-flow thermoelectric air-to-air heat pump unit

The configuration of the proposed cross-flow thermoelectric heat pump unit is shown in Figure 3. The proposed heat pump unit has two main air streams, which are not mixed with each other. When direct current is applied to the TEM, inlet 1 air is heated and inlet 2 is cooled. The proposed heat pump unit was composed of a thermoelectric module and flat-fin heat sinks, which comprise the air path channel for sensible heat transfer. The dimensions of the heat sinks were 198×198×40 mm with 31 fins, and the number of total heat sinks was four (with inlet 1 and inlet 2 each having two heat sinks). The dimensions of the fins were 198×20×2 mm and the dimensions of the base plate, which serves to distribute the heat evenly, was 198×198×20 mm. TEMs with a size of 40×40×3.8 mm were used, and the number of TEMs in the proposed system was 27, with 9 being arranged in a grid in each layer and the spacing between TEMs being 40 mm. The circuit was constructed so that the same current intensity was applied to all the TEMs. The TEM specifications are described in Table 1. Because a single TEM has a heating capacity of 50 W, the proposed system has a total heating capacity of ~1.4 kW. The overall dimensions of the proposed system were 440×440×200 mm.

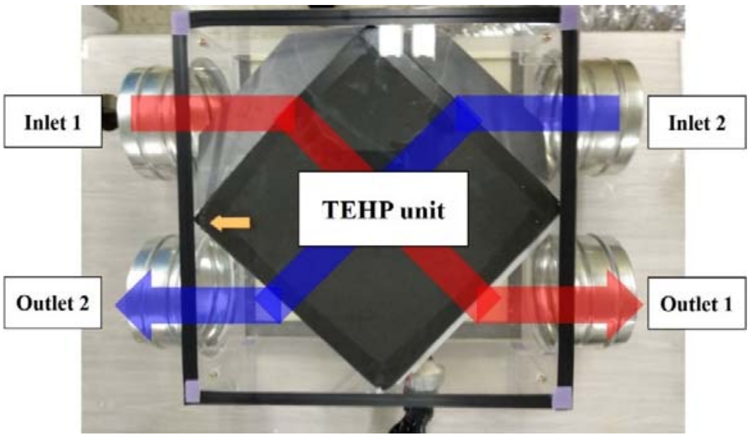

Figure 3: Configuration of a cross-flow thermoelectric air-to-air heat pump unit

Figure 4 shows the detailed configuration of the proposed unit. There are a total of 136 air channels, with 68 at each inlet part; the size of the rectangular channels is 6.8×20 mm. An air guide line was installed at the inlets to prevent the formation of vortices, which would interrupt the flow of air. To prevent thermal interference between heating and cooling at the baseplate, insulation was installed between the TEMs. To reduce contact resistance between the TEMs and the heat sink (baseplate), thermal grease was applied to each side of the TEM surface, and bolts were tightened to integrate the system. K-type temperature sensors were inserted in the middle of the TEM layer, and nine sensors were attached to the top and bottom of the TEMs.

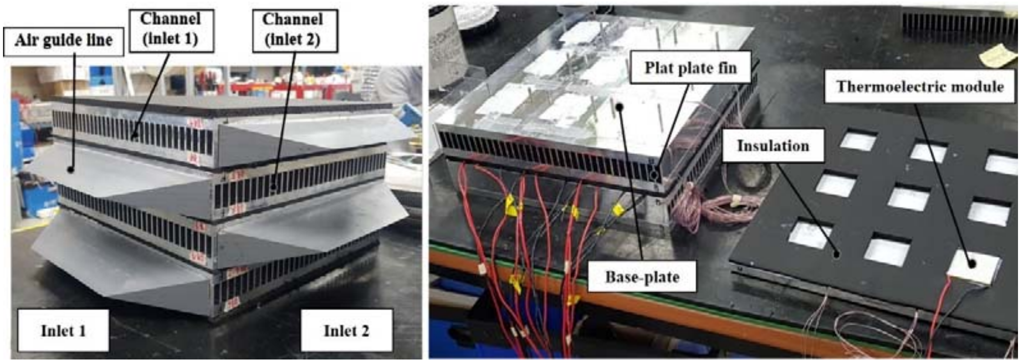

Figure 4: Configuration of the inlet side (left) and inside of the thermoelectric air-to-air heat pump unit (right)

Table 1: Characteristics of the TEM

Model	I_{max}	V_{max}	Q_{max}	ΔT_{max}
HMN6040MCX	6.4 A	14.4 V	56 W ($T_h = 25$°C)	77°C

3. EXPERIMENTAL SETUP AND HEAT EXCHANGE EFFECTIVENESS

3.1 Experimental setup of cross-flow thermoelectric air-to-air heat pump unit

To analyze the performance of the TEHP unit, we constructed the experimental setup shown in Figure 5. To determine the performance of the TEHP unit, we adjusted the air temperature, air flow, and current. Air conditioning systems were used to maintain the two inlet air temperatures, and the humidity air condition was maintained to prevent condensation. That is, heat exchange between air and the TEMs was configured for only sensible heat exchange. To reduce the influence of the external thermal environment, insulation was attached to the duct and TEHP unit. The volume flow rates supplying inlet 1 and inlet 2 were controlled through frequency control of a variable fan. The input current, which is applied to the TEM, was controlled by a switched mode power supply (SMPS). The SMPS is able to supply constant current and voltage to the TEM.

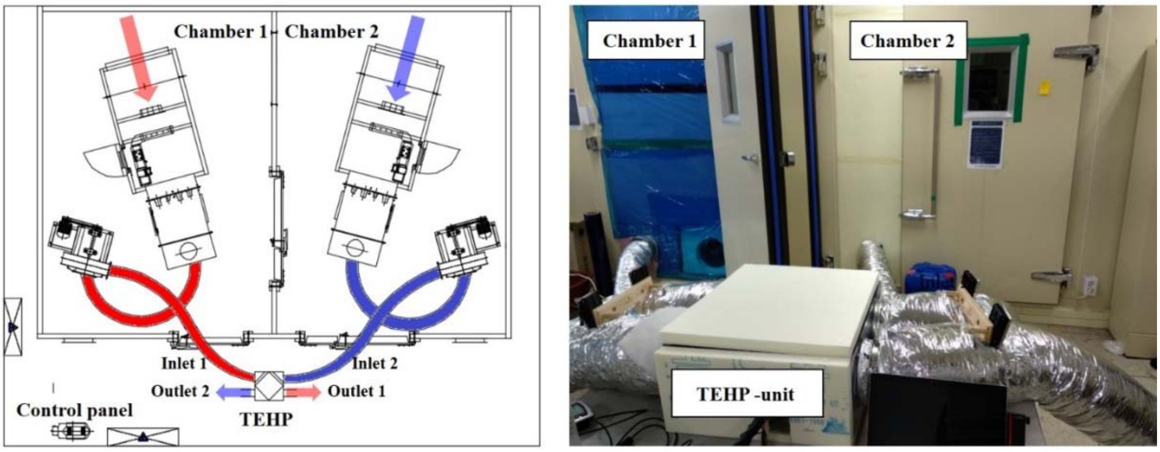

Figure 5: Schematic diagram of the experimental setup (left) and a photograph of the thermoelectric heat pump unit (right)

3.2 Experimental conditions and instruments

In this study, 35 sets of experiments were conducted for analyzing the heat exchange effectiveness of the cross-flow thermoelectric air-to-air heat pump unit. The heat exchange effectiveness of the TEHP unit represents the heat transfer between the surface of the heat sink and the incoming air to the channel, and the heat exchange effectiveness of the hot- and cold-side channels, respectively, were derived. The values of the heat exchanger effectiveness of the hot and cold sides are defined as the ratio of the actual heat transfer of the air passing through the TEHP unit under ideal conditions:

$$\varepsilon_h = \frac{T_{a,out1} - T_{a,in1}}{T_{h,sur} - T_{a,in1}}, \tag{4}$$

$$\varepsilon_c = \frac{T_{a,out2} - T_{a,in2}}{T_{a,in2} - T_{h,sur}}. \tag{5}$$

The data were used to analyze the heat exchange effectiveness at both channels with respect to five operating parameters: the temperatures of inlet 1 and inlet 2, the air flow rates of inlet 1 and inlet 2, and the current intensity supplied to the TEM. Table 2 lists the operating range of the inlet parameters to the TEHP unit. To demonstrate the heat exchange effectiveness of the TEHP unit under various input conditions (temperature, flow rate, and current), each variable was adjusted.

Inlet and outlet dry bulb temperatures were measured by using a high-precision humidity/temperature probe. The volume flow rate was measured by using differential pressure sensors and was regulated by frequency control, which was adjusted by a control panel. The surface temperature of the TEMs was measured by using a K-type sensor and a thermocouple. Table 3 describes the measurement equipment range and accuracy, respectively, for the air temperature and humidity sensors, air flow rate sensor, and surface temperature of the TEM sensors.

Table 2: Operating ranges of the experimental conditions

Parameter	**Symbol**	**Input values**	
		Low	High
Inlet 1 air temperature [°C]	$T_{a,in1}$	5	50
Inlet 2 air temperature [°C]	$T_{a,in2}$	24	24
Inlet 1 air flow rate $[m^3/h]$	$\dot{V}_{a,in1}$	150	330
Inlet 2 air flow rate $[m^3/h]$	$\dot{V}_{a,in2}$	100	210
Current intensity [A]	I_{TEM}	1	3.6

Table 3: Specifications of measuring instruments

Variable	**Device**	**Characteristics**		
Dry-bulb temperature and relative humidity of air	High-precision humidity/temperature probe	Range	Temperature	−20℃ to +55℃
			Relative humidity	0%–100%
		Accuracy	Temperature	±0.4℃
			Relative humidity	±2%RH
Air flow rate	Differential pressure sensor	Range	Pressure	0–1250 Pa
		Accuracy		±0.30%
TEM surface temperature	T-type immersion temperature probe	Range	Temperature	−200℃ to 400℃
		Accuracy		±0.5℃

4. EXPERIMENTAL RESULTS AND DISCUSSION

The influences of the air inlet parameters (inlet 1 air temperature, inlet 2 air temperature, inlet 1 volume flow rate, and inlet 2 volume flow rate) and current on the heat exchange effectiveness, surface temperature of the TEM, and outlet temperature were experimentally investigated. The influence of each of the five factors on the heat exchange effectiveness and surface temperature of the TEM and outlet temperature was analyzed. In this paper, we focused on influence of the current and volume flow rate on the heat exchange effectiveness.

The influence of the current and volume flow rate on the temperature distribution and heat exchange effectiveness are shown in Figures 6 and 7, respectively. Figure 6 shows that the temperature distribution of six variables (inlet 1, inlet 2, outlet 1, outlet 2, top surface, and bottom surface) and heat exchange effectiveness according to current intensity. The temperature difference between hot and cold surface temperatures becomes larger as the current into the TEM increases. The supplied temperature of inlet 1 and inlet 2 was 24℃ and the volume flow rates of inlet 1 and inlet 2 were 200 and 330 m^3/h, respectively. For a current of 3.6 A, the cold surface temperature is higher than that for a current at 3 A because the heat on hot side could not dissipate. The heat exchange effectiveness of hot and cold sides ranged from 0.41 to 0.52 and from 0.23 to 0.31, respectively. Figure 7 shows the temperature distribution of six variables and the heat exchange effectiveness according to the volume flow rate. The temperature difference between hot and cold sides for a 1 A current was 14℃ to 16℃. As the airflow of the hot side increases, the temperature of the hot and cold surfaces decreased. Thus, the hot-side heat exchange effectiveness decreased while the cold-side heat exchange effectiveness increased. The heat exchange effectiveness of hot and cold sides ranged from 0.41 to 0.59 and from 0.23 to 0.30, respectively.

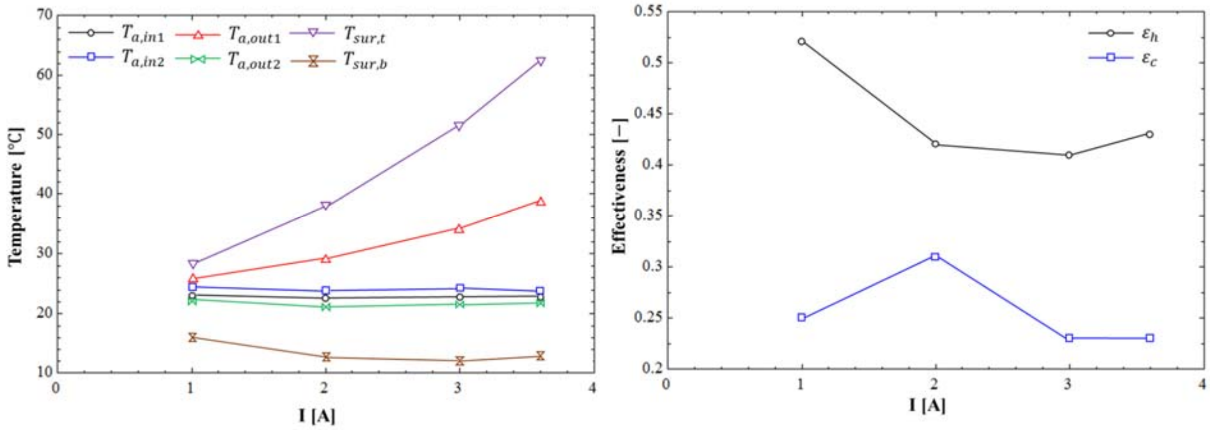

(a) Temperature distribution according to current change

(b) Heat exchange effectiveness of hot and cold sides according to current change

Figure 6: Influence of current on the thermoelectric heat pump unit

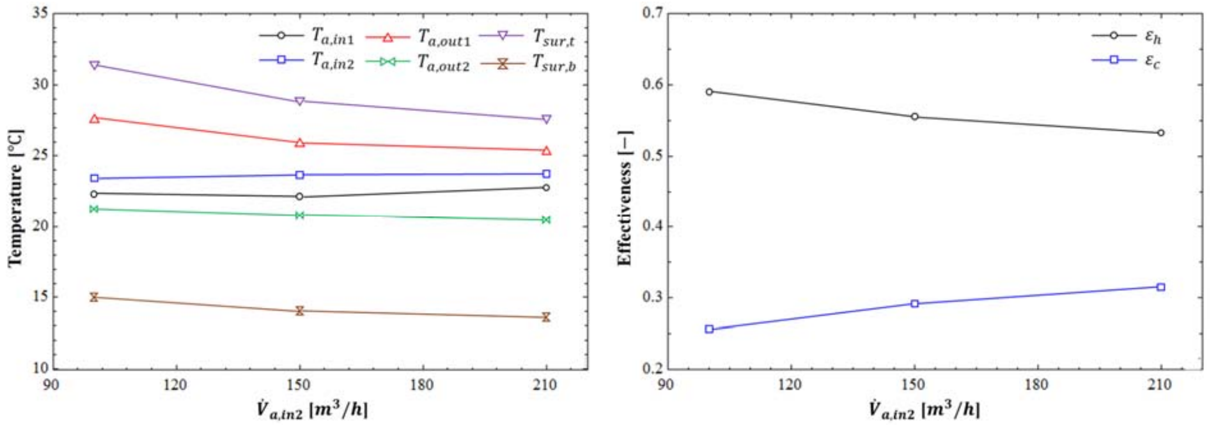

(a) Temperature distribution under a 1 A current condition

(b) Heat exchange effectiveness of hot and cold sides under a 1 A current condition

Figure 7: Influence of volume flow rate on the thermoelectric heat pump unit

In Figure 8 shows the results of the temperature change of six parameters with time. The volume flow rates of inlet 1 and inlet 2 are both 200 m^3/h, and the supplied temperatures of inlet 1 and inlet 2 are 40℃ and 25℃, respectively. When a current of 1 A is supplied to the positive input, the top surface temperature increases from 36.1℃ to 46.7℃ and the bottom surface temperature drops from 31.5℃ to 24.4℃. When a current of 3 A is supplied, the hot-side heat is not dissipated by air, the surface temperature of the heat absorption part is increased, and the air temperature is not further cooled. When a current of 1 A is supplied to the negative input, the top surface temperature drops from 37.2℃ to 28.8℃ and the bottom surface temperature increases from 32.2℃ to 41.9℃. The results show that the direction of the electric flow easily switches the hot and cold parts and that the thermal response is high.

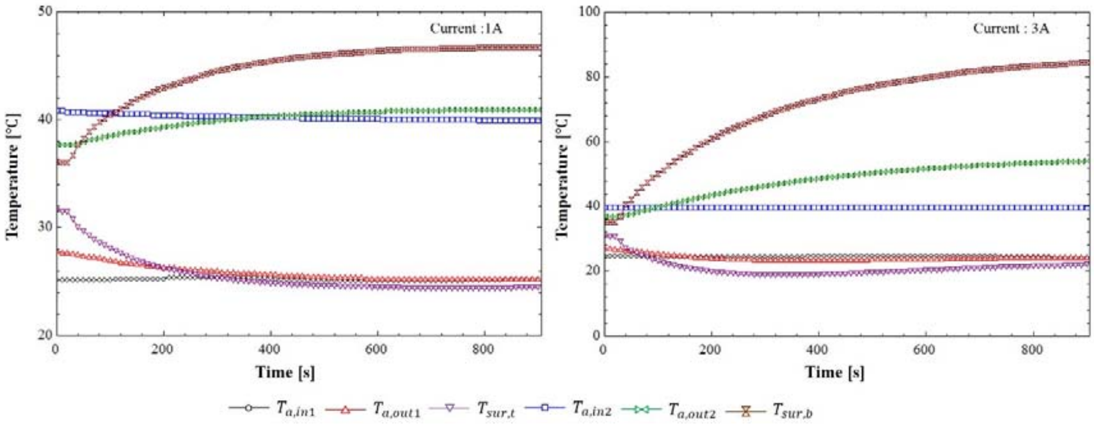

(a) Temperature distribution with a 1 A current to the positive input

(b) Temperature distribution with a 3 A current to the positive input

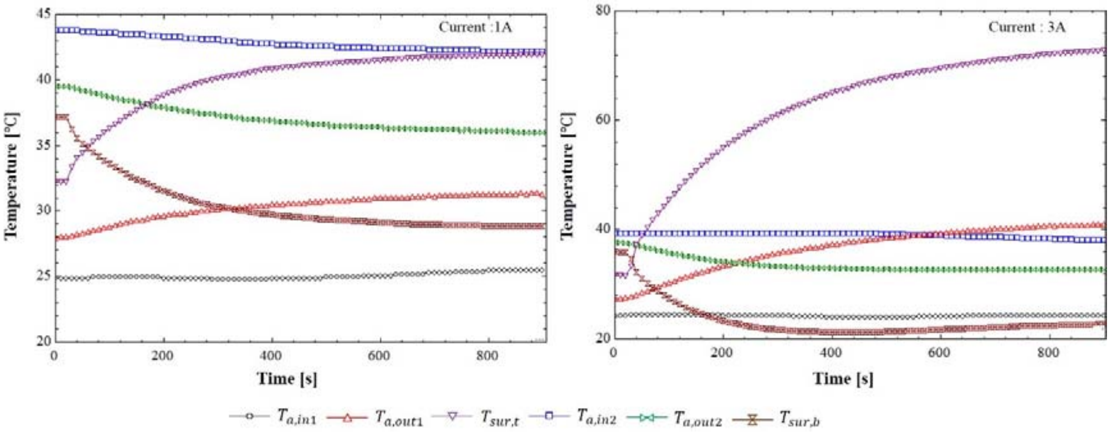

(c) Temperature distribution with a 1 A current to the negative input

(d) Temperature distribution with a 3 A current to the negative input

Figure 8: Performance of the thermoelectric heat pump unit over time

5. CONCLUSIONS

In this study, we experimentally investigated the heat exchange effectiveness of a cross-flow thermoelectric air-to-air heat pump unit. The proposed system is composed of a flat-plate fin array that is heat exchanger integrated TEM for cooling and heating. Experiments were conducted to predict the cooling and heating heat exchange effectiveness by collecting performance data. Design parameters had a significant impact on the heat exchange effectiveness of the flat-plate heat exchanger integrated TEM for air cooling and heating. The influence of five input parameters (air temperature at both side, air flow rate at both side, and current) were analyzed. In the proposed unit, the heat exchange effectiveness of hot and cold sides ranged from 0.41 to 0.59 and from 0.23 to 0.30, respectively. Thus, the heat-transfer efficiency between the hot-side surface and the incoming air is higher than that of cold-side part. The heat exchange effectiveness of the hot side has a tendency to be larger than that of the cold side. The maximum temperature difference between hot and cold surfaces was 53℃ when the current supply was 3.6 A.

In future studies, we will analyze the effect of heat exchange efficiency on the heat quantity, COP, power amount, and heat sink shape of the proposed system and further develop an empirical model to expand the utilization of the air-to-air thermoelectric heat pump.

NOMENCLATURE

Q	heat transfer	(W)
S	Seebeck coefficient	(V/K)
I	current	(A)
R	electric resistance	(Ω)
K	thermal conductivity	(W/K)
T	temperature	(℃)
P	power of thermoelectric module	(W)

Greek Symbol

ε	Heat exchange effectiveness	(-)

Subscripts

h	hot
c	cold
a	air
sur	surface
t	top
b	bottom

REFERENCES

Al-Nimr, M.A., Tashtoush, B.M., Jaradat, A.A. (2015). Modeling and simulation of thermoelectric device working as a heat pump and an electric generator under Mediterranean climate. *Energy*, 90, 1239–1250.
Shen, L., Xiao, F., Chen, H., Wang, S. (2013). Investigation of a novel thermoelectric radiant air-conditioning system. *Energy and Buildings*, 59, 123–132.
Irshad, K., Habib, K., Basrawi, F., Saha, B.B. (2017). Study of a thermoelectric air duct system assisted by photovoltaic wall for space cooling in tropical climate. *Energy*, 119, 504–522.
Li, T., Tang, G., Gong, G., Zhang, G., Li, N., Zhang, L. (2009). Investigation of prototype thermoelectric domestic-ventilator. *Applied Thermal Engineering*, 29, 2016–2021.
Kim, Y.W., Ramousse, J., Fraisse, G., Dalicieux, P., Baranek, P. (2014). Optimal sizing of a thermoelectric heat pump (THP) for heating energy-efficient buildings. *Energy and Buildings*, 70, 106–116.
Yilmazoglu, M.Z. (2016). Experimental and numerical investigation of a prototype thermoelectric heating and cooling unit. *Energy and Buildings*, 113, 51–60.
Lim, H.S., Cheon, S.Y., Jeong, J.W. (2018). Empirical analysis for the heat exchange effectiveness of a thermoelectric liquid cooling and heating unit. *Energies*, 11(3), 580.

ACKNOWLEDGMENT

This work was supported by a Korea Agency for Infrastructure Technology Advancement (KAIA) grant (17CTAP-C116268-02) and the Korea Institute of Energy Technology Evaluation and Planning (KETEP) (No. 20164010200860).